Noninvasive Multimodality Imaging of the Tumor Microenvironment: Registered Dynamic 1H MRI and 18F PET Studies of a Preclinical Model of Tumor Hypoxia.

H. Cho[1], E. Ackerstaff[1], S. Carlin[1], M. Lupu[1], Y. Wang[1], A. Rizwan[1], J. O'Donoghue[1], C. Ling[1], J. Humm[1], P. Zanzonico[1], and J. Koutcher[1]

[1]Memorial Sloan Kettering Cancer Center, New York, NY, United States

Introduction: Improved understanding and the ability to image specific important features of the tumor microenvironment *in vivo* will provide important prognostic information about tumors and factors that induce responses or resistance to treatment [1,2]. In this study, multimodality *in vivo* Magnetic Resonance Imaging (MRI) and Positron Emission Tomography (PET) imaging using stereotactic fiduciary markers [3] in the Dunning R3327-AT prostate tumor was performed, focusing on the relationship between Dynamic Contrast-Enhanced (DCE)-MRI using Magnevist® (Gd-DTPA), and dynamic ^{18}F-fluoromisonidazole (^{18}F-Fmiso) PET. The non-invasive measurements were verified using tumor tissue sections stained for haematoxylin/eosin (H&E), pimonidazole and ^{18}F digital autoradiography.

Materials and Methods: Animal studies were conducted in compliance with protocols approved by the Institutional Animal Care and Use Committee (IACUC) of Memorial Sloan-Kettering Cancer Center (MSKCC). The rat prostate cancer cell line R3327-AT was cultured and two to four million R3327-AT cells were injected in the right hind leg of 6~8 weeks-old Copenhagen rats. The MRI coil and fiduciary marker assembly were built for MRI and PET image registration. The DCE-MRI experiments were performed on a Bruker 7T BioSpin (Bruker, Germany) imaging spectrometer. T_1-weighted DCE-MRI (FLASH, TR=33 ms, TE=3.1 ms, NR=256, NA=1, st=0.79 mm, number of slices =4, FOV=3.5 cm x 3.5 cm, matrix= 128*128, flip angle: 30^o) was performed with a 5.47s temporal resolution and in-plane resolution of 273 μ m x 273 μ m in plane. The contrast agent Gd-DTPA was injected via the tail vein after 2 minutes of baseline acquisition followed by 20 minutes of dynamic acquisition. For PET studies, the MRI markers were replaced with catheter tubings filled with ^{18}F-Fmiso diluted with red dye to an activity of ~10 μ Ci/ml. MicroPET Focus 120 (CTI Molecular Imaging, Inc., Knoxville, TN) was used for dynamic PET imaging (2~3 hours) immediately after the injection of ^{18}F-Fmiso (1.5 mCi) and pimonidazole. After the PET scan, the animal was then sacrificed in place by isoflurane overdose, three catheters with steel needles were pushed through the holes of the histology marker disk into the tumor, and the tumor excised with catheter-histology disk assembly in place. The resulting catheter-histology disk-tumor assembly, frozen down in OCT,,ensured the co-registration of tissue sections with the *in vivo* MR and PET images. MRI and PET images were co-registered using fiduciary marker system and both time activities curves are analyzed using Matlab for voxel-by-voxel analysis for the correlation studies [4,5].

Results: Fig. 1A and 1B show the DCE-MRI time-signal curves and ^{18}F-Fmiso PET time-activity curves for a representative voxel for perfused, hypoxic, and necrotic regions, respectively selected from corresponding DCE-MRI Akep map, pimonidazole, and H&E staining. In the DCE-MR study, the T_1-weighted proton signal increased fastest in the non-necrotic area, as a result of rapid Gd-DTPA uptake in the well-perfused region followed by rapid washout. In contrast, hypoxic regions, typically characterized by reduced vascularization, showed a delayed Gd-DTPA uptake corresponding to a delay in signal build-up and also to a delay in washout (Fig. 1A). In necrotic regions of the tumor, the time-dependent increase in the MR signal was slowest and no washout could be observed for the duration of the MR experiment. In ^{18}F-Fmiso PET studies, well-perfused areas of the tumor were likewise characterized by rapid initial increase of ^{18}F-Fmiso activity which subsequently decreased at later times. Hypoxic areas of the tumor demonstrated lower initial activity than well-perfused areas of the tumor but continued to accumulate further ^{18}F-Fmiso during the time course of the experiment, as manifested by the distinctive positive slope (Fig. 1B). In Fig. 2, the relationship between DCE Akep map (A) and early ^{18}F-Fmiso uptake values (B) and late ^{18}F-Fmiso slope (C) for tumors of varying size are shown. The voxel-by-voxel scatterplot demonstrated positive correlations (R: 0.5~0.7, Fig. 2D-1, D-2) The regions of positive slopes in late ^{18}F-Fmiso PET appeared mainly in the less perfused areas and there were negative correlations (R~-0.35) between DCE-MRI Akep and the late slope ^{18}F-Fmiso PET curves (Fig. 5C-1, C-2, E-1, E-2).

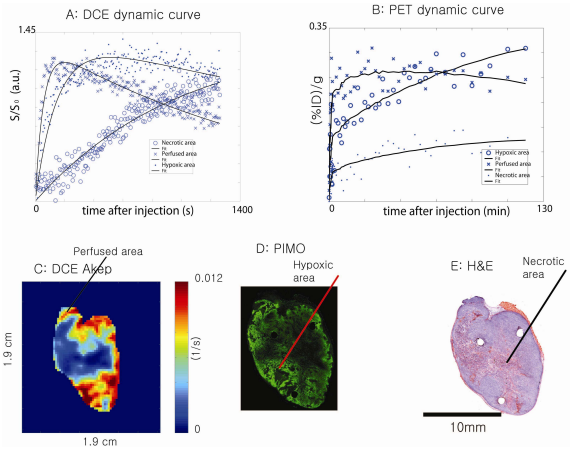

Figure 1. Characteristic dynamic uptake curves of Gd-DTPA-assisted DCE-MRI (A) and ^{18}F-Fmiso PET (B) for different tumor microenvironments.

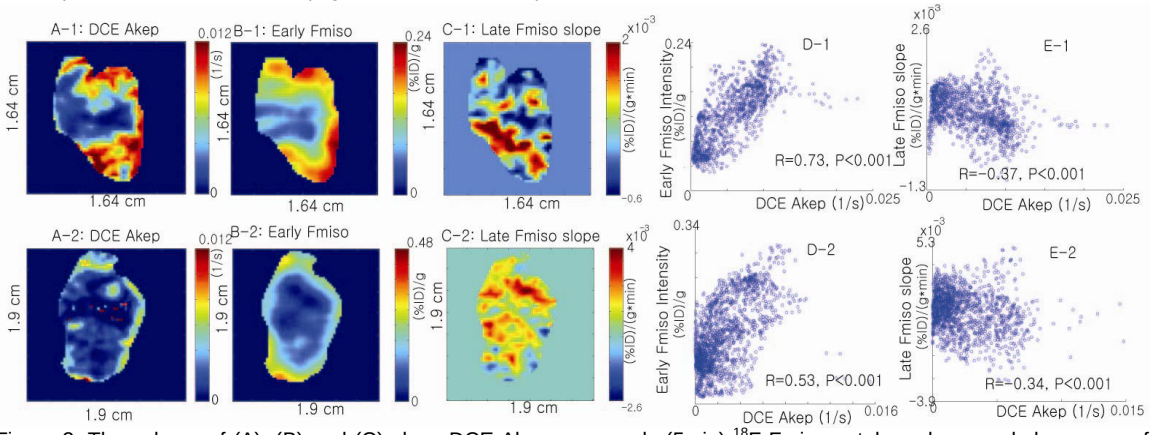

Figure 2. The column of (A), (B) and (C) show DCE-Akep map, early (5min) ^{18}F-Fmiso uptake values, and slope map of later ^{18}F-Fmiso curve for a slice from two different animals, respectively. The columns of (D) and (E) plot voxel-by-voxel scatterplot for the direct comparison of these quantities.

Conclusions: The relationship between DCE-MRI and H&E slice, ^{18}F-miso PET and pimonidazole slice respectively confirms the validity of MRI/PET measurement to image the tumor microenvironment. DCE Akep values (perfusion markers) with respect to early uptake and late slope map of ^{18}F-Fmiso PET (hypoxia marker) showed positive and negative correlations, respectively.

References : [1] N.Chaudary et al. (2006). *Breast Diseases* **26**, 55-64, [2] M. Hockel, et al. (1996) *Semin Radiation Oncology* **6**, 3-9. [3] J.L.Humm et al.(2003) *Med.Phys* **30**, 2303-2314. [4] U.Hoffmann et al. (1995). *Magnetic Resonance in Medicine* **33**, 506-514.[5] D.Thorwarth, et al.(2005). *Phys. Med. Biol* **50**, 2209-2224.